

The Effect of Biradical Concentration on the Performance of DNP-MAS-NMR

Sascha Langea^{a,1}, Arne H. Linden^{a,1}, Ümit Akbey^a, W. Trent Franks^a, Nikolaus M. Loening^b,
Barth-Jan van Rossum^a, Hartmut Oschkinat^{a,*}

^aFMP, Leibniz-Institut für Molekulare Pharmakologie, Robert-Rössle-Str. 10, 13125 Berlin, Germany

^bDepartment of Chemistry, Lewis & Clark College, 0615 S.W. Palatine Hill Road, Portland, Oregon 97219, USA

*Corresponding author

¹Equally contributing authors

Keywords: Dynamic Nuclear Polarization, TOTAPOL, Biradical, Solid State NMR,

With the technique of dynamic nuclear polarization (DNP) signal intensity in solid-state MAS-NMR experiments can be enhanced by 2-3 orders of magnitude. DNP relies on the transfer of electron spin polarization from unpaired electrons to nuclear spins. For this reason, stable organic biradicals such as TOTAPOL are commonly added to samples used in DNP experiments. We investigated the effects of biradical concentration on the relaxation, enhancement, and intensity of NMR signals, employing a series of samples with various TOTAPOL concentrations and uniformly ¹³C, ¹⁵N labeled proline. A considerable decrease of the NMR relaxation times (T_1 , T_2^* , and $T_{1\rho}$) is observed with increasing amounts of biradical due to paramagnetic relaxation enhancement (PRE). For nuclei in close proximity to the radical, decreasing $T_{1\rho}$ reduces cross-polarization efficiency and decreases in T_2^* broaden the signal. Additionally, paramagnetic shifts of ¹H signals can cause further line broadening by impairing decoupling. On average, the combination of these paramagnetic effects (PE; relaxation enhancement, paramagnetic shifts) quenches NMR-signals from nuclei closer than 10 Å to the biradical centers. On the other hand, shorter T_1 times allow the repetition rate of the experiment to be increased, which can partially compensate for intensity loss. Therefore, it is desirable to optimize the radical concentration to prevent additional line broadening and to maximize the signal-to-noise observed per unit time for the signals of interest.

1. Introduction

Solid-state nuclear magnetic resonance is a widely used method for structural analysis of inherently insoluble systems, like membrane proteins [1-3] and fibrils [4-6]. The intrinsically low sensitivity of this technique can be enhanced by the use of cross polarization (CP) [7] and magic-angle spinning (MAS) [8]. Nevertheless, for many biological investigations sensitivity is still the limiting factor. In 1953, Overhauser proposed transferring the relatively large electron Boltzmann polarization of an unpaired electron spin to a nuclear spin [9]; a method known as dynamic nuclear polarization (DNP) [10]. DNP has been shown in several cases to enhance the signal intensity by two to three orders of magnitude in MAS-NMR experiments [11-14]. To achieve DNP in solid-state MAS experiments, stable free organic radicals are added to the sample as a source of unpaired electrons and spectra are measured under continuous microwave irradiation at cryogenic temperatures [15]. Biradicals with a defined range of distances between their two unpaired electrons were developed to take advantage of a particularly efficient three-spin polarization transfer mechanism at high magnetic fields [16]. It has been shown that the polarization enhancement is further distributed via spin diffusion processes throughout the sample [11]. One prominent example of such a biradical is TOTAPOL [17], which has become widely used in biological studies utilizing DNP [18].

2. Experiment

In this paper, we investigate the effects of the TOTAPOL concentration (c_T) in the range of 15 to 196 mM on the DNP-MAS-NMR spectra of uniformly ¹³C, ¹⁵N-labeled (CN) samples of proline. We dissolved CN proline in a buffer containing 60%

glycerol-d₈, 30% D₂O, and 10% H₂O to a concentration of 50 mM, which corresponds to 1.25 μmol of analyte in a 25 μL rotor. These concentrations correspond to biradical/analyte ratios of between 0.3 and 3.92 and are comparable to the concentrations used in biological DNP applications. All experiments were performed using a Bruker Avance III 400 MHz wide-bore spectrometer equipped with a Bruker 264 GHz gyrotron as a microwave source and a Bruker triple resonance DNP probe. All spectra were recorded at a MAS frequency of 8889 Hz and a sample temperature of 101 K. The sample temperature was measured with ⁷⁹Br following the method of Thurber and Tycko [19]. We used TPPM proton decoupling with a field strength of 100 kHz. The same field was used for the proton 90° pulse. ¹³C hard pulses and ¹³C CP pulses were applied with a field strength of 62.5 kHz. The ¹H CP field strength was optimized to match the Hartmann-Hahn condition with a linear ramp (75% to 100%) from proton to carbon. The acquisition time was always set to 25 ms. For the various samples with different c_T we determined the proton T_1 relaxation times and calculated the optimum recycle delay accordingly ($1.3 \cdot T_1$).

3. Results and Discussion

One-dimensional proton-carbon CP ¹³C spectra were recorded with either a constant number of scans (Figure 1A) or a constant total experiment time (Figure 1B). The signal-to-noise ratio (S/N) for a constant number of scans decreases with c_T . In contrast, the S/N for a constant experiment time reaches a maximum at a c_T of 26 mM and then decreases with further increases of c_T . In the following we analyze the dependence of the relaxation times, line width, DNP signal enhancement (ϵ), and S/N on c_T . The presence of radicals significantly reduces the bulk spin-lattice relaxation times (T_1) of the nuclei. Without

TOTAPOL the ^1H T_1 of proline in solution at 100 K is 27.8 s. With 15 mM of biradical the ^1H T_1 is reduced to 5.4 s and with 26 mM to 2.7 s (Figure 2A). A short T_1 enables a faster repetition rate in proton-carbon CP experiments, leading to an increased S/N per unit time. The S/N reaches a maximum around a c_T of 26 mM in experiments measured within a constant total experiment time (Figure 1B). For the sake of comparison, we calculated the sensitivity (κ) following the definition given by Ernst et al. [20] as S/N per square root of measurement time (taking into account that the optimal recycle delay equals 1.3 times the proton T_1) and sample amount in the rotor as follows:

$$\kappa = \frac{S/N}{n_A \cdot \sqrt{T_1} \cdot n_S \cdot 1.3}$$

n_A = analyte per rotor in μmol
 n_S = number of scans

In the system investigated, κ ranged from 1 to 15.8, depending on the c_T used; without DNP κ was 0.15 (Figure 2B). The biradical also leads to a shortening of the spin-spin relaxation time (T_2^*) of the nuclei of interest, especially for the presented case of a frozen solution of small molecules. Although shorter values of T_2^* correlate with broader lines, for cryogenic samples this homogeneous broadening can be masked by inhomogeneous broadening [21]. No change in linewidth is detected between c_T 's of 0 and 26 mM, which represents the commonly used range of biradical concentrations (Figure 2A). Additionally, we measured T_2^* at a low (26 mM) and a very high (196 mM) c_T . The calculated theoretical minimum linewidth at half height ($w_{1/2} = 1/(\pi T_2^*)$) are 1.6 ppm and 5.3 ppm, respectively. The measured linewidths for these c_T (3.9 and 7.5 ppm) are, as expected, larger, most probably due to insufficient decoupling and inhomogeneous line broadening. However, if the radical is spatially separated from the spins of interest, as expected for protein preparations, it is possible to observe narrow lines (as shown in Barnes *et al.* [22]). Additionally, this has been shown in the case of a neurotoxin bound to nACh-receptors in membranes, where the reduction of the biradical close to the analyte leads to well resolved spectra. [23] Variation of c_T also influences the spin-lattice relaxation time in the rotating frame ($T_{1\rho}$). As the CP contact time (t_{cp}) of a ^1H to ^{13}C CP step needs to be smaller than $T_{1\rho}$ of the protons [24], high c_T can lead to a significant decrease in CP transfer efficiency for long contact times. To analyze this effect, we measured the CP efficiency as a function of t_{cp} , which should show a significant decrease when t_{cp} exceeds the proton $T_{1\rho}$ (Figure 3). At a c_T of 15 mM the CP efficiency stays nearly unchanged for t_{cp} between 100 and 1000 μs . At a c_T of 52 mM, which is approximately the upper limit of common usage, the CP-efficiency reaches a maximum for a t_{cp} of 100 μs and drops to 63% of its maximum at 1000 μs . With a c_T of 196 mM the signal integral of the 1D ^1H - ^{13}C CP spectra decreases from its maximum at a t_{cp} of 50 μs to only 6% at 1000 μs . It is important to note that pulse sequences with several CP steps will yield better results at even lower c_T values than the "optimal" c_T that we found (26 mM) because the signal loss across a series of CP steps is multiplicative.

Radicals may broaden signals beyond detection due to paramagnetic relaxation enhancement (PRE) [22,25,26]. Furthermore, at high c_T the radical can induce large paramagnetic shifts of proton resonances. This can lead to less efficient proton de-

coupling [27], which causes additional line broadening due to incomplete decoupling. In the following, both effects (PRE and paramagnetic shifts) are discussed as paramagnetic effects (PE). These PE reduce the signal intensities of both the DNP enhanced and the non-enhanced spectra. Past DNP studies have looked at the enhancement factor, which is the ratio between the enhanced and non-enhanced signal for a sample with a given c_T . As PE affect both the enhanced and non-enhanced signals, the effects cancel and are consequently masked. Hence, the dependence of the enhancement factor on c_T shows a broad maximum followed by a gradual decay. This gradual decay in the enhancement factor is caused by electron-electron interactions between the radical molecules (Figure 2B). The sensitivity, on the other hand, depends on the PE. Therefore, κ drops more rapidly than the enhancement factor at higher c_T . We modeled the volume of molecules affected by PE as overlapping cylinders with spherical caps, referred to as rods, surrounding each TOTAPOL molecule (Figure 4A, B). In this model, we simplified the r^{-6} distance dependence of PRE by defining the radii of the rods as the cut-off distance in which all signals are quenched [25]. To this end, we calculated the bleached volume V_{bN} covered by N overlapping rods to be:

$$V_{bN} = \sum_{i=1}^N B_i$$

where B_i is the volume occupied by rod i :

$$B_i = V_m + (V_s \cdot a_i)$$

Here, V_m is the impenetrable volume of one TOTAPOL molecule. Each molecule is surrounded by a penetrable rod-shaped volume V_s , representing the PE affected region, corrected by a factor a , taking into account overlapping.

$$a_i = \left(\frac{V - (i \cdot V_m) - \sum_{j=1}^{i-1} D_j}{V - (i \cdot V_m)} \right)$$

with

$$D_j = V_s \cdot a_j \quad \parallel j < i$$

As described in Melnyk et al. [28] it is also possible to approximate the filling of a volume with penetrating rods using an simplified model:

$$V_r = V - V_{bN} \approx V - e^{-k \cdot c_T}$$

V_r is the residual unoccupied volume and κ is a factor proportional to the radius r of the spheres surrounding each radical center. We calculated k for different values of r and plotted this set of functions against the biradical concentration. On the basis of the measured signal integrals we approximated the bleached volume (Figure 4). Comparing the model and the measured data we estimated that, on average, all signals from nuclei closer than 10 Å to a radical center are bleached due to the PE (Figure 4). For example, at a c_T of 50 mM, only 48% of the nuclei are detectable in both enhanced and unenhanced spectra. The approximated radius is in agreement with effective PRE-distances from literature [25].

In summary, we have shown that for DNP-enhanced NMR the biradical concentration needs to be chosen carefully to achieve optimal sensitivity. In particular, the enhancement factor *alone* is not a sufficient criterion for the DNP benefit. The different effects of c_T on the performance of DNP-MAS-NMR experiments, some of which act against one another, demand a sample specific *and* experiment-specific compromise. Large biradical concentrations lead to greater enhancements and allow for fast repetition rates – both of which enhance sensitivity – but reduce the number of detectable nuclei and create larger line widths – both of which reduce sensitivity. These findings are in line with recent investigations by DNP enhanced ^{29}Si NMR spectroscopy [29] and the effects of different radicals and their concentrations on the enhancement of solvent signals at very low temperatures [30]. From our data it is expected that experiments with several CP steps or measurements of long-range distances will suffer the most at higher biradical concentrations. We determined that for a sample of proline, a c_T of around 25 mM is a good compromise. At this concentration, the sensitivity in a 1D experiment is at a maximum, losses due to a decreased CP efficiency are still small, and the effects on the line width are negligible. Interpolating the observed tendencies towards the situation in protein samples, we need to consider the character of the proline sample used here. Most importantly, proteins are large. Consequently, one may see residual sharp signals at high c_T for nuclei that are distant from the surface and hence are always more than 10 Å away from the radical. In such case, biradical concentrations greater than 25 mM may lead to a maximum S/N for the signals of interest in the core of the protein. As other investigations on biological systems show, the optimal concentration can be in the range of 6 to 50 mM depending on the system [11,15,17,30-33]. This communication presents important experimental considerations for DNP-MAS-NMR and will help to further improve a system specific sample preparation.

References

- [1] F. Creuzet, A. McDermott, R. Gebhard, K. van der Hoef, M.B. Spijker-Assink, J. Herzfeld, J. Lugtenburg, M.H. Levitt, R.G. Griffin, *Science* 251 (1991) 783–786.
- [2] F.M. Marassi, A. Ramamoorthy, S.J. Opella, *Proc. Natl Acad. Sci. USA* 94 (1997) 8551–8556.
- [3] M. Hiller, L. Krabben, K.R. Vinothkumar, F. Castellani, B.-J. van Rossum, W. Kühlbrandt, H. Oschkinat, *ChemBioChem* 6 (2005) 1679–1684.
- [4] A.T. Petkova, Y. Ishii, J.J. Balbach, O.N. Antzutkin, R.D. Leapman, F. Delaglio, R. Tycko, *Proc. Natl Acad. Sci. USA* 99 (2002) 16742–16747.
- [5] C. Wasmer, A. Lange, H. van Melckebeke, A.B. Siemer, R. Riek, B.H. Meier, *Science* 319 (2008) 1523–1526.
- [6] H. Heise, W. Hoyer, S. Becker, O.C. Andronesi, D. Riedel, M. Baldus, *Proc. Natl Acad. Sci. USA* 102 (2005) 15871–15876.
- [7] A. Pines, M.G. Gibby, J.S. Waugh, *Chem. Phys. Lett.* 15 (1972) 373–376.
- [8] M. Maricq, J. Waugh, *J. Chem. Phys.* 70 (1979) 3300–3316.
- [9] A.W. Overhauser, *Phys. Rev.* 92 (1953) 411–415.
- [10] D.A. Hall, D.C. Maus, G.J. Gerfen, S.J. Inati, L.R. Becerra, F.W. Dahlquist, R.G. Griffin, *Science* 276 (1997) 930.
- [11] P.C.A. van der Wel, K.-N. Hu, J. Lewandowski, R.G. Griffin, *J. Am. Chem. Soc.* 128 (2006) 10840–10846.
- [12] V.S. Bajaj, M.L. Mak Jurkauskas, M.L. Belenky, J. Herzfeld, R.G. Griffin, *Proc. Natl Acad. Sci. USA* 106 (2009) 9244–9249.
- [13] M. Rosay, V. Weis, K. Kreisler, R. Temkin, *J. Am. Chem. Soc.* 124 (2002) 3214–3215.
- [14] U. Akbey, W.T. Franks, A. Linden, S. Lange, R.G. Griffin, B.-J. van Rossum, H. Oschkinat, *Angew. Chem. Int. Ed.* 49 (2010) 7803–7806.
- [15] K.-N. Hu, H.-H. Yu, T.M. Swager, R.G. Griffin, *J. Am. Chem. Soc.* 126 (2004) 10844–10845.
- [16] Y. Matsuki, T. Maly, O. Ouari, H. Karoui, F. Le Moigne, E. Rizzato, S. Lyubenova, J. Herzfeld, T. Prisner, P. Tordo, R.G. Griffin, *Angew. Chem. Int. Ed.* 48 (2009) 4996–5000.
- [17] C. Song, K.-N. Hu, C.-G. Joo, T.M. Swager, R.G. Griffin, *J. Am. Chem. Soc.* 128 (2006) 11385–11390.
- [18] M. Rosay, L. Tometich, S. Pawsey, R. Bader, R. Schauwecker, M. Blank, P.M. Borchard, S.R. Cauffman, K.L. Felch, R.T. Weber, R.J. Temkin, R.G. Griffin, W.E. Maas, *Phys. Chem. Chem. Phys.* 12 (2010) 5850–5860.
- [19] K.R. Thurber, R. Tycko, *J. Magn. Reson.* 196 (2009) 84–87.
- [20] R.R. Ernst, G. Bodenhausen, A. Wokaun, *Principles of Nuclear Magnetic Resonance in One and Two Dimensions*, Oxford University Press, 1990.
- [21] A.H. Linden, W.T. Franks, U. Akbey, S. Lange, B.-J. van Rossum, H. Oschkinat, *J. Biomol. NMR* 51 (2011) 283–292.
- [22] A.B. Barnes, B. Corzilius, M.L. Mak Jurkauskas, L.B. Andreas, V.S. Bajaj, Y. Matsuki, M.L. Belenky, J. Lugtenburg, J.R. Sirigiri, R.J. Temkin, J. Herzfeld, R.G. Griffin, *Phys. Chem. Chem. Phys.* 12 (2010) 5861–5867.
- [23] A.H. Linden, S. Lange, W.T. Franks, U. Akbey, E. Specker, B.-J. van Rossum, H. Oschkinat, *J. Am. Chem. Soc.* 133 (2011) 19266–19269.
- [24] S. Hartmann, E. Hahn, *Phys. Rev.* 128 (1962) 2042–2053.
- [25] G.M. Clore, J. Iwahara, *Chem. Rev.* 109 (2009) 4108–4139.
- [26] N. Bloembergen, *Physica* 15 (1949) 386–426.
- [27] A. Brough, C. Grey, C. Dobson, *J. Am. Chem. Soc.* 115 (1993) 7318–7327.
- [28] T. Melnyk, J. Rowlinson, *J. Comput. Phys.* 7 (1971) 385–393.
- [29] A.J. Rossini, A. Zagdoun, M. Lelli, D. Gajan, F. Rascón, M. Rosay, W.E. Maas, C. Copéret, A. Lesage, L. Emsley, *Chem. Sci.* 3 (2011) 108.
- [30] K.R. Thurber, W.-M. Yau, R. Tycko, *J. Magn. Reson.* 204 (2010) 303–313.
- [31] T. Maly, A.-F. Miller, R.G. Griffin, *ChemPhysChem* 11 (2010) 999–1001.
- [32] V. Vitzthum, M.A. Caporini, G. Bodenhausen, *J. Magn. Reson.* 205 (2010) 177–179.
- [33] A. Lesage, M. Lelli, D. Gajan, M.A. Caporini, V. Vitzthum, P. Miéville, J. Alauzun, A. Roussey, C. Thieuleux, A. Mehdi, G. Bodenhausen, C. Copéret, L. Emsley, *J. Am. Chem. Soc.* 132 (2010) 15459–15461.

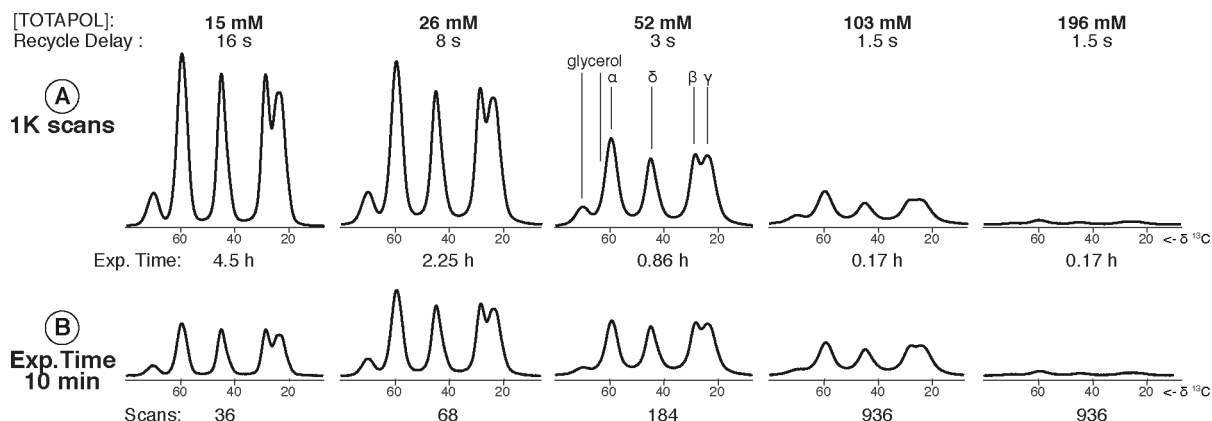


Figure 1: 1D ^1H - ^{13}C CP spectra of uniformly ^{13}C , ^{15}N -labeled proline with varying concentrations of TOTAPOL recorded (A) with 1024 scans and (B) with an experiment time as close to 10 min as possible in each case. The recycle delay was adjusted to the longest measured proton- T_1 times (except for the sample with 196 mM TOTAPOL because of probe duty cycle limitations). All spectra were recorded using a zirconium rotor with Vespel® cap at 100 K with a CP contact time of 500 μs and an acquisition time of 25 ms. All spectra were processed without window functions and plotted at the same noise level.

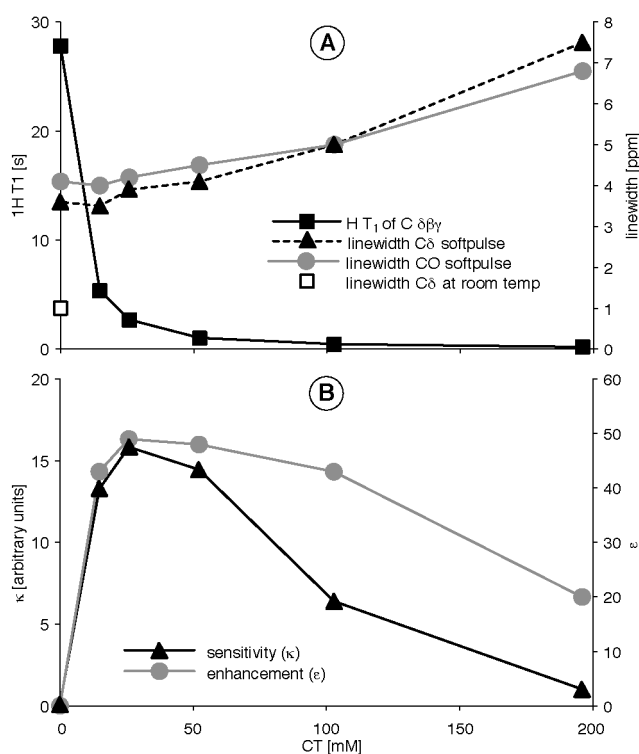


Figure 2: A. Proton- T_1 relaxation times (left axis; filled squares); line-width at half high of the δ -carbon (right axis; triangles) and of the carbonyl-carbon (right axis; circles) with application of a soft pulse as measured with samples containing 50 mM ^{13}C , ^{15}N -labeled proline and different c_T ; the additional value at 0 mM TOTAPOL (open square) was measured with a 120 mg natural abundance proline sample at room temperature. B. Sensitivity of the δ -carbon peak (κ , left axis; triangles) and DNP enhancements (right axis; circles) of ^{13}C , ^{15}N -labeled proline. All data points were measured with 1D CP spectra recorded with a contact time of 500 μs .

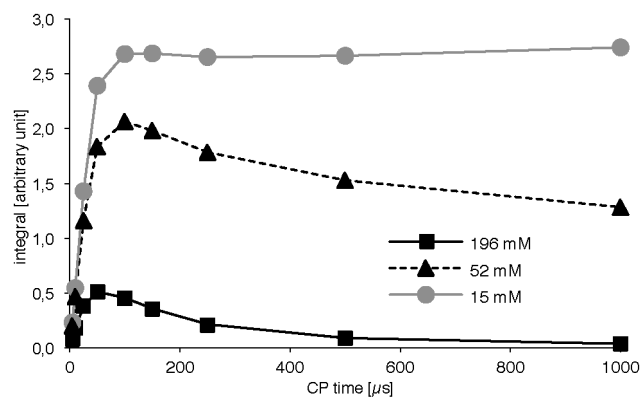


Figure 3: Proton CP efficiency at different contact times and for different concentrations of TOTAPOL. The corresponding 1D spectra of ^{13}C , ^{15}N -labeled proline were measured with 128 scans at 100 K. The recycle delay was adjusted according to the measured proton T_1 times except for the highest c_T (196 mM) where a longer recycle delay was used due to probe duty cycle limitations.

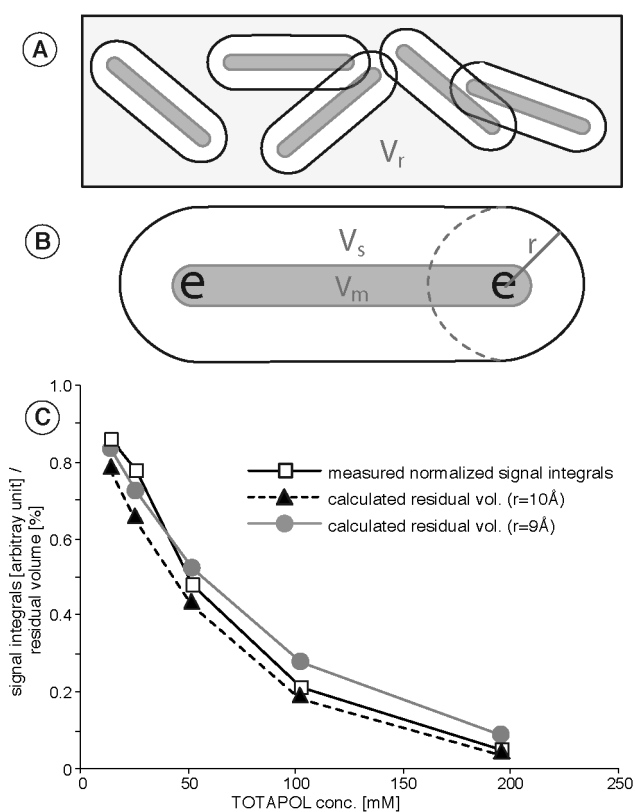


Figure 4: **A.** TOTAPOL molecules are surrounded by rod-shaped volumes in this model, wherein PE makes the NMR signals undetectable. **B.** These rods can overlap and partially fill the sample volume. **C.** Normalized signal integrals (open squares) for a constant number of scans as measured with a sample of 50 mM ^{13}C , ^{15}N -labeled proline and calculated residual unoccupied volumes (V_r , see also text) for a 3.2 mm rotor filled with TOTAPOL molecules, surrounded by overlapping rod-shaped volumes with radius 9 Å (filled circles) and 10 Å (filled triangles), respectively.